Chaotic advection induced by a magnetic chain in a rotating magnetic field

T.G. Kang, M.A. Hulsen, P.D. Anderson, J.M.J. den Toonder and H.E.H. Meijer

Materials Technology, Eindhoven University of Technology
PO Box 513, 5600MB Eindhoven, The Netherlands
E-mail: t.g.kang@tue.nl

ABSTRACT

We investigated chaotic advection induced by a magnetic chain in a two-dimensional circular cavity under the influence of a rotating magnetic field. Our focus is on the dynamics of the chain and the route to induce chaotic mixing. A direct simulation method based on the Maxwell stress tensor and a fictitious domain method is employed to solve magnetic and flow problems in a coupled manner. The motion of the chain is significantly affected by the Mason number, the ratio of viscous force to magnetic force. At a lower Mason number, the chain rotates like a rigid body following the field. Alternating break-up and reformation of the chain are observed within a limited range of the Mason number, which induce two typical flows: a single rotating flow and two co-rotating flows. From a series of deformation patterns of a blob, we found that the two alternating flows result in enhanced mixing, showing an exponential increase of the interfacial length.

Keywords: chaotic advection, magnetic chain, rotating magnetic field, fictitious domain method, Maxwell stress tensor

1 INTRODUCTION

In microfluidic systems, magnetic particles are used as mobile substrates for bio-assays to be transported to a desired location or as stirring agents to achieve enhanced mixing [1,2]. As a fundamental study of chaotic mixing by a magnetic chain, we aim to investigate the dynamics of the chain and subsequent mixing under the influence of a rotating magnetic field. With this purpose in mind, we developed a direct numerical simulation method enabling us to take into account both hydrodynamic and magnetic interactions in a fully coupled manner. The flow problem with rigid particles is solved using a fictitious domain [3] and the finite element method. The forces due to an applied magnetic field and interactions between particles are implemented through the Maxwell stress tensor. As a model problem we choose a two-dimensional circular cavity with suspended circular particles initially forming a chain in the applied magnetic field. The motion of the chain and enhanced mixing by topological changes such as break-up and reformation of the chain will be discussed with an emphasis on the effect of the Mason number, the ratio of the viscous force to the magnetic force.

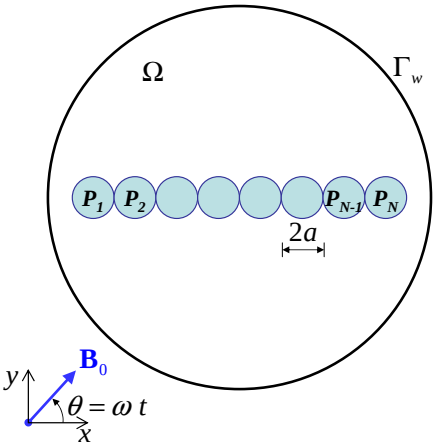

Figure 1: Schematic representation of a magnetic chain in a two-dimensional circular cavity under the influence of a rotating magnetic field.

2 MODELING

2.1 Problem definition

As depicted in fig. 1, the problem chosen is a flow in a two-dimensional circular cavity with N circular particles initially forming a chain aligned horizontally. The magnetic flux density $\boldsymbol{B}_0$, which is the only driving force to move the particles and induce flow, has the form

$$\boldsymbol{B}_0 = B_0(\cos(\omega t)\boldsymbol{e}_x + \sin(\omega t)\boldsymbol{e}_y), \qquad (1)$$

where ω is the angular frequency of the rotating field and t the time. The fluid is assumed to be non-magnetic with the magnetic permeability μ_0 and the viscosity η. The particles are circular with the same radius a and are assumed to have a constant permeability μ_p. The fluid flow is assumed to be governed by viscous forces and magnetic interactions between particles, neglecting the effect of inertia.

NSTI-Nanotech 2007, www.nsti.org, ISBN 1420061844 Vol. 3, 2007

2.2 Magnetostatic problem

We assume that the magnetic field is governed by magnetostatics, for which the governing Maxwell's equations can be written as

$$\nabla \times \boldsymbol{H} = \boldsymbol{J}, \tag{2}$$

$$\nabla \cdot \boldsymbol{B} = 0, \tag{3}$$

where $\boldsymbol{H}$ is the magnetic field intensity, $\boldsymbol{J}$ the current density, and $\boldsymbol{B}$ the magnetic flux density. The constitutive equation relating $\boldsymbol{B}$ and $\boldsymbol{H}$ is $\boldsymbol{B} = \mu \boldsymbol{H}$, where μ denotes the magnetic permeability of a linear isotropic medium.

In general, to solve the magnetostatic Maxwell's equations, the first-order partial differential equations are converted into second-order partial differential equations involving only one field variable called the magnetic vector potential $\boldsymbol{A}$ [4]. In a two-dimensional Cartesian coordinate system, the governing equation in terms of the magnetic vector potential becomes

$$-\frac{\partial}{\partial x}\left(\frac{1}{\mu_r}\frac{\partial A}{\partial x}\right) - \frac{\partial}{\partial y}\left(\frac{1}{\mu_r}\frac{\partial A}{\partial y}\right) = \mu_0 J, \tag{4}$$

where μ_r, A, and J denote the relative permeability and the z-components of $\boldsymbol{A}$ and $\boldsymbol{J}$, respectively. Once the magnetic potential A is found, the components of the magnetic flux density, $\boldsymbol{B} = (B_x, B_y)$, are computed by

$$B_x = \frac{\partial A}{\partial y}, \quad B_y = -\frac{\partial A}{\partial x}. \tag{5}$$

The body force $\boldsymbol{f}_m$ experienced by materials in a magnetic field is represented by the divergence of the Maxwell stress tensor $\boldsymbol{T}_m$, i.e. $\boldsymbol{f}_m = \nabla \cdot \boldsymbol{T}_m$, where $\boldsymbol{T}_m = \mu(\boldsymbol{H}\boldsymbol{H} - \frac{1}{2}H^2\boldsymbol{I})$.

2.3 Flow problem

We assume that the fluid flow is governed by the Stokes equations and the particles are force-free, torque-free, and inertialess. For the fluid domain $\Omega \backslash P(t)$, the set of equations describing fluid flow are represented by

$$-\boldsymbol{\nabla} \cdot \boldsymbol{\sigma} = \nabla \cdot \boldsymbol{T}_m \quad \text{in } \Omega \backslash P(t), \tag{6}$$

$$\boldsymbol{\nabla} \cdot \boldsymbol{u} = 0 \quad \text{in } \Omega \backslash P(t), \tag{7}$$

$$\boldsymbol{\sigma} = -p\boldsymbol{I} + 2\eta \boldsymbol{D} \quad \text{in } \Omega \backslash P(t), \tag{8}$$

$$\boldsymbol{u} = \boldsymbol{U}_i + \boldsymbol{\omega}_i \times (\boldsymbol{x} - \boldsymbol{X}_i) \quad \text{on } \partial P_i(t) \ (i = 1, ..., N), \tag{9}$$

$$\boldsymbol{u} = \boldsymbol{0} \quad \text{on } \Gamma_w, \tag{10}$$

where $\boldsymbol{\sigma}$ is the Cauchy stress tensor, $\boldsymbol{T}_m$ the Maxwell stress tensor, $\boldsymbol{u}$ the velocity, p the pressure, η the viscosity, $\boldsymbol{D}$ the rate-of-deformation tensor, $\boldsymbol{U}_i$ the translational velocity of the i-th particle, $\boldsymbol{\omega}_i$ the angular velocity of the i-th particle, $\boldsymbol{x}$ the position vector of a point on the i-th particle boundary, and $\boldsymbol{X}_i$ the position vector of the center of the i-th particle. Equations (6), (7), and (8) are the momentum balance equation, the continuity equation and the constitutive relation for the fluid domain, respectively. Equations (9) and (10) are the constraints for rigid body motion of the particles and the essential boundary condition at the solid wall, respectively.

As for the particle domain $P(t)$, we employ the rigid ring description in [5] where the same fluid as the fluid domain also fills the particle domain and the rigid body motion is imposed on the particle boundaries only. This description enables us to solve the same governing equations for both (fluid and particle) domains, reducing the number of unknowns for the rigid body constraints.

3 NUMERICAL METHODS

3.1 Magnetostatic problem

The weak form for the Poisson equation, Eq. (4), for the magnetic potential A is given as: find $A \in \mathbb{S}$ such that

$$\int_\Omega \frac{1}{\mu_r}\left(\nabla A \cdot \nabla \psi\right) dA = \int_\Omega \mu_0 J dA, \tag{11}$$

for all $\psi \in \mathbb{S}_0$ with $\mathbb{S} = \{A \in H^1(\Omega) \text{ with } A = \bar{A} \text{ at } \Gamma_w\}$ and $\mathbb{S}_0 = \{\psi \in H^1(\Omega) \text{ with } \psi = 0 \text{ at } \Gamma_w\}$. The weak form is used to obtain an approximate solution using the finite element method with bi-quadratic interpolation for A. The resulting matrix equation is solved using HSL/MA57, a sparse multi-frontal Gauss elimination method to solve a symmetric matrix [6].

3.2 Flow problem

In this section, we present only the final weak formulation (for the detailed procedure of derivation we refer to [3,5]). In the combined weak formulation, the rigid body constraint is enforced by the constraint equation using a Lagrange multiplier, $\boldsymbol{\lambda}^{p,i}$, defined on the particle boundary ∂P_i. For a given particle configuration $\boldsymbol{X}_i (i = 1, ..., N)$, the weak form for the entire domain Ω can be stated as follows: find $(\boldsymbol{u}, \boldsymbol{U}_i, \boldsymbol{\omega}_i) \in \mathbb{V}$, $p \in \mathbf{L}^2(\Omega)$, and $\boldsymbol{\lambda}^{p,i} \in \mathbf{L}^2(\partial P_i(t))$ $(i = 1, \ldots, N)$ such that

$$\begin{aligned} &\int_\Omega 2\eta \boldsymbol{D}(\boldsymbol{u}) : \boldsymbol{D}(\boldsymbol{v}) dA - \int_\Omega p \nabla \cdot \boldsymbol{v} dA \\ &+ \sum_{i=1}^{N} \left\langle \boldsymbol{\lambda}^{p,i}, \boldsymbol{v} - (\boldsymbol{V}_i + \boldsymbol{\chi}_i \times (\boldsymbol{x} - \boldsymbol{X}_i)) \right\rangle_{\partial P_i} \\ &= -\int_\Omega \boldsymbol{T}_m : \boldsymbol{D}(\boldsymbol{v}) dA, \end{aligned} \tag{12}$$

$$\int_\Omega q \nabla \cdot \boldsymbol{u} dA = 0, \tag{13}$$

$$\langle \boldsymbol{\mu}^{p,i}(\boldsymbol{x}), \boldsymbol{u}(\boldsymbol{x}) - (\boldsymbol{U}_i + \boldsymbol{\omega}_i \times (\boldsymbol{x} - \boldsymbol{X}_i)) \rangle_{\partial P_i} = 0, \tag{14}$$

for all $(\boldsymbol{v}, \boldsymbol{V}_i, \boldsymbol{\chi}_i) \in \mathbb{V}$, $q \in L^2(\Omega)$, and $\boldsymbol{\mu}^{p,i} \in L^2(\partial P_i(t))$ $(i = 1, \ldots, N)$. We use bi-quadratic interpolation for the velocity and bi-linear for the pressure. The resulting matrix equation is solved by HSL/MA57.

3.3 Interface tracking

To track the interface of a blob (as a tool visualizing the progress of mixing), we employed an adaptive interface tracking method [7]. This method makes it possible to accurately track interfaces experiencing exponential stretching in the case of chaotic advection.

4 RESULTS

4.1 Scaling analysis

First, we introduce the result of scaling analysis for the momentum balance equation, Eq. (6), aiming to extract dimensionless parameters influencing the motion of the chain and the fluid flow. Non-dimensional variables (with a superscript *) are given by

$$x^* = \frac{x}{l_c}, \quad y^* = \frac{y}{l_c}, \tag{15}$$

$$\boldsymbol{u}^* = \frac{\boldsymbol{u}}{u_c}, \tag{16}$$

$$p^* = \frac{p}{p_c}, \tag{17}$$

$$T_{ij}^* = \frac{T_{ij} - \mu_0 H_c^2}{(\mu_p - \mu_0) H_c^2}, \tag{18}$$

where l_c denotes a characteristic length, $\boldsymbol{u}_c$ a characteristic velocity, p_c a characteristic pressure, and H_c the characteristic magnetic field intensity. Here we define the characteristic length, velocity and pressure as $l_c = a$, $u_c = a/t_c$ and $p_c = \eta u_c/a$, respectively. The Maxwell stress tensor T_{ij} is non-dimensionalized by the stress difference (with the reference being $\mu_0 H_c^2$) normalized by $(\mu_p - \mu_0)H_c^2$. The characteristic time scale is defined as $t_c = \omega^{-1}$. The characteristic magnetic field intensity is defined as $H_c = H_0 = B_0/\mu_0$. Then, the resulting non-dimensional momentum equation is

$$\nabla^* p^* - \nabla^{*2} \boldsymbol{u}^* = \frac{1}{\mathrm{Ma}} \nabla^* \cdot \boldsymbol{T}^*, \tag{19}$$

where Ma is the Mason number, which is the ratio of the viscous force to the magnetic force under the influence of a rotating magnetic field, defined by

$$\mathrm{Ma} = \frac{\eta \omega}{\mu_0 \chi_\mathrm{p} H_0^2}, \tag{20}$$

with χ_p being the magnetic susceptibility of the particle.

4.2 Chain motion and flow characteristics

We carry out simulations at three Mason numbers, Ma=0.001, 0,002, and 0.003, to investigate the dynamics of a magnetic chain and flow characteristics. In the simulations, we fixed the ratio of particle radius and cavity radius to be $a/R_c = 0.05$, so the area fraction of the particles equals $\phi_a = 0.0425$ with the number of particles $N = 17$. The cavity is discretized into 14400 nine-node rectangular elements. The time step used is 0.02 in non-dimensional units.

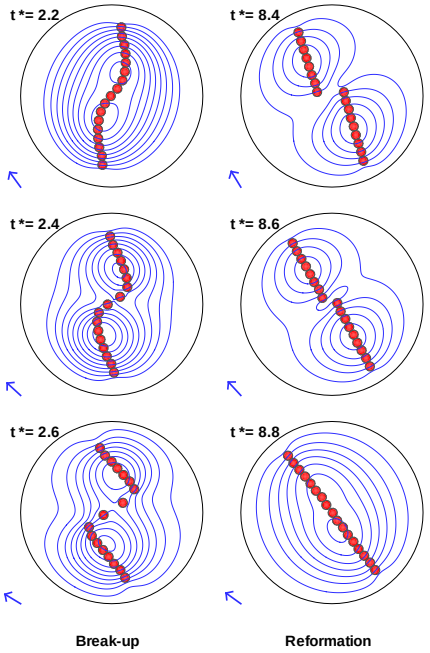

Figure 2: Streamlines and chain configurations at the moment of chain break-up and reformation at Ma=0.002. The arrow indicates the direction of the magnetic field.

Depicted in fig. 2 are deformation patterns of the chain and streamlines at the moment of break-up and reformation of the chain with Ma=0.002. The representative flow characteristics determined by the configuration of the chain are two typical flows: one with a single rotating flow and the other with two co-rotating flows. The shape of chain at break-up is quite similar to that observed experimentally by Melle *et al* [8]. The hyperbolic flow at break-up is thought to be a key mechanism of mixing together with the rotational motion the chain, leading to stretching and folding. As shown in fig. 3, the motion of the chain is significantly influenced by the Mason number. At Ma=0.001, the chain rotates almost like a rigid body following the magnetic field, but with a phase lag behind the rotating field. We observe break-up of the chain at both Ma=0.002 and 0.003. The difference between the two chain motions at Ma=0.002 and 0.003 is whether the detached chains form a single chain again or remain as separate chains without joining together. At Ma=0.003, once the chain is broken the two resulting chains induce only two co-rotating flows, which is less effective as a mixing protocol than the former where the two flows are taking place in an alternating manner.

NSTI-Nanotech 2007, www.nsti.org, ISBN 1420061844 Vol. 3, 2007

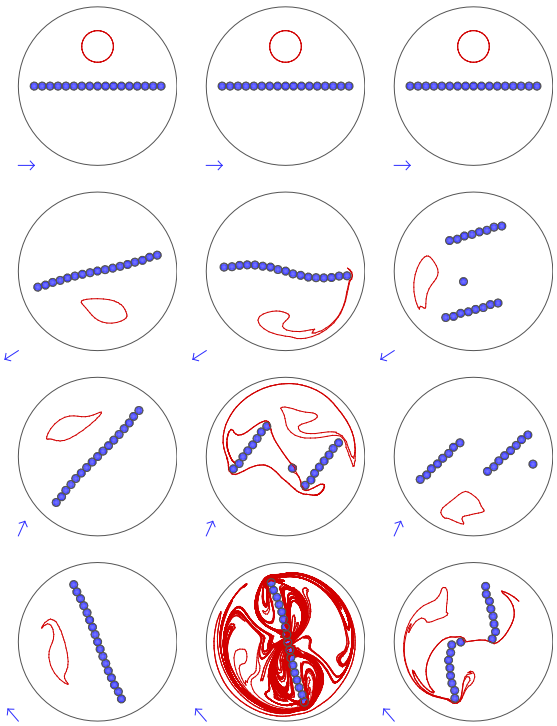

Figure 3: Chain dynamics and deformation of a circular material blob of radius 0.1 initially positioned at (0.5,0.75) for the three Mason numbers, (a) Ma=0.001, (b) Ma=0.002 and (c) Ma=0.003. The radius of the circular cavity is 0.5 with its center at (0.5,0.5). The evolution of the blob is plotted at the non-dimensional time $t^* = 0$, 10, 20, and 40 (from top).

4.3 Mixing analysis

We tracked the interface of a circular passive blob of the fluid in time. Figure 3 shows the motion of the chain and the evolution of the blob at the three Mason numbers, Ma=0.001, 0.002, and 0.003, with their initial configuration illustrated in the first row. From a series of deformation patterns of the blob shown in fig. 3, we found that alternating break-up and reformation of the chain at Ma=0.002 results in the best mixing among the three. We also characterized mixing by the length stretch of the blob (see fig. 4). The length stretch is defined as $\lambda = l(t^*)/l_0$, where $l(t^*)$ is the interfacial length of the blob at time t^* and l_0 is the initial interfacial length. The length stretch at Ma=0.002 increases faster than for the others due to stretching and folding induced by the alternating topological changes of the chain. Given cavity size, particle size, and particle area fraction (in the 2D case), the motion of the chain and subsequent mixing are significantly affected by the Mason number.

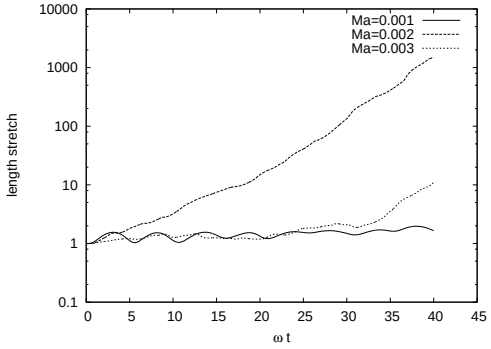

Figure 4: Length stretch λ of the blob at Ma=0.001, 0.002, and 0.003. The abscissa is the non-dimensional time $t^* = \omega t$.

5 CONCLUSION

We investigated chaotic advection induced by a magnetic chain, formed by magnetic particles, in a rotating magnetic field. A direct simulation method based on the Maxwell stress tensor and a fictitious domain method has been successfully applied to solve flows with a suspended magnetic chain in a two-dimensional circular cavity. Our numerical method enables us to take into account both hydrodynamic and magnetic interactions in a fully coupled manner. The motion of the chain and the fluid flow are significantly affected by the Mason number. At Ma=0.002, we observe alternating break-up and reformation of the chain, which lead to an exponential increase of the interfacial length by stretching and folding. The two alternating flow portraits, a single rotating flow and two co-rotating flows induced by the topological changes of the chain, are key factors for effective mixing.

REFERENCES

[1] A. Rida and M.A.M. Gijs, Anal. Chem., 76(21), 6239–6246, 2004.
[2] R. Calhoun, A. Yadav, P. Phelan, A. Vuppu, A. Garciab and M. Hayes, Lab. Chip., 6, 247–257, 2006.
[3] R. Glowinski, T.W. Pan, T.I. Hesla and D.D. Joseph, Int. J. Multiphase Flow, 25(5), 755–794, 1999.
[4] J. Jin, "The Finite Element Method in Electromagnetics," John Wiley & Sons Inc., New York, 2002.
[5] W.R. Hwang, M.A. Hulsen and H.E.H. Meijer, J. Comput. Phys., 194(2), 742–772, 2004.
[6] HSL, http://www.numerical.rl.ac.uk/hsl, 2002.
[7] O.S. Galaktionov, P.D. Anderson, G.W.M. Peters and F.N. van de Vosse, Int. J. Numer. Methods Fluids, 32(2), 201–217, 2000.
[8] S. Melle, O.G. Calderon, M.A. Rubio and G.G. Fuller, Phys. Rev. E, 68, 041503–1–041503–11, 2003